Journal of Solid State Chemistry 181 (2008) 2401–2405

Contents lists available at ScienceDirect

Journal of Solid State Chemistry

journal homepage: www.elsevier.com/locate/jssc

One-step synthesis of hydrothermally stable mesoporous aluminosilicates with strong acidity

Dongjiang Yang [a,b], Yao Xu [a,*], Dong Wu [a], Yuhan Sun [a]

[a] Chinese Academy of Sciences, State Key Laboratory of Coal Conversion, Institute of Coal Chemistry, Taiyuan 030001, China
[b] School of Physical and Chemical Sciences, Queensland University of Technology, Brisbane, QLD 4001, Australia

ARTICLE INFO

Article history:
Received 31 January 2008
Received in revised form
19 May 2008
Accepted 25 May 2008
Available online 6 June 2008

Keywords:
Mesoporous materials
Nonsurfactant routine

ABSTRACT

Using tetraethylorthosilicate (TEOS), polymethylhydrosiloxane (PMHS) and aluminium isopropoxide (AIP) as the reactants, through a one-step nonsurfactant route based on PMHS–TEOS–AIP co-polycondensation, hydrothermally stable mesoporous aluminosilicates with different Si/Al molar ratios were successfully prepared. All samples exclusively showed narrow pore size distribution centered at 3.6 nm. To assess the hydrothermal stability, samples were subjected to 100 °C distilled water for 300 h. The boiled mesoporous aluminosilicates have nearly the same N_2 adsorption–desorption isotherms and the same pore size distributions as those newly synthesized ones, indicating excellent hydrothermal stability. The ^{29}Si MAS NMR spectra confirmed that PMHS and TEOS have jointly condensed and CH_3 groups have been introduced into the materials. The ^{27}Al MAS NMR spectra indicated that Al atoms have been incorporated in the mesopore frameworks. The NH_3 temperature-programmed desorption showed strong acidity. Due to the existence of large amount of CH_3 groups, the mesoporous aluminosilicates obtained good hydrophobicity. Owing to the relatively large pore and the strong acidity provided by the uniform four-coordinated Al atoms, the excellent catalytic performance for 1,3,5-triisopropylbenzene cracking was acquired easily. The materials may be a profitable complement for the synthesis of solid acid catalysts.

1. Introduction

Mesoporous aluminosilicates have attracted much recent attention because of their potential applications in heterogeneous catalysts and catalyst supports, especially for large molecule catalysis [1,2]. However, the poor hydrothermal stability and weak acid strength relative to the conventional zeolites, limited their applications in petroleum refining and fine-chemical production [1]. Several approaches have been aimed at improving these properties. For example, Mokaya et al. [3–6] have prepared mesoporous aluminosilicates with hydrothermal stability via post-synthesis treatments such as grafting of Al onto the pore walls or recrystallization of pure silica materials in the presence of aluminium precursor. Pinnavaia et al. [7,8] and Xiao et al. [2,9] have successfully assembled hydrothermally stable and strongly acidic mesoporous aluminosilicates using protozeolitic seeds. In our group, hydrothermally stable mesoporous aluminosilicates with tubular morphology have also been synthesized via the controlled coassembly of protozeolitic nanoclusters and soluble species [10]. Herein, using as a basis of the nonsurfactant route provided in our previous works [11–13], hydrothermally stable mesoporous aluminosilicates with strong acidity were prepared via a one-step synthesis, which may be a profitable complement for the synthesis of solid acid catalysts.

2. Experimental section

Tetraethylorthosilicate (TEOS, 99%, Acros), polymethylhydrosiloxane (PMHS, 99%, MW = 2700–5400, Acros) and aluminium isopropoxide (AIP, 98%, Acros) were used as the reactants without further purification. A typical one-step synthesis procedure for the hydrothermally stable mesoporous aluminosilicate was as follows: 2.338 g of PMHS and 4.676 g of TEOS (at a PMHS/TEOS mass ratio of 1:2) were mixed in 70 mL anhydrous ethanol (pH = 10, adjusted by NaOH solid) under a vigorous stirring for 24 h. Then determined AIP (at a Si/Al molar ratio of 25 and 50) and deionized water were added to the above mixture. After stirring for 3 h, the solution was aged for 4–5 d and finally turned into gel. The obtained gels were heated in a 60 °C vacuum oven to remove the solvent, and were designated as ASM25 and ASM50 corresponding to the Si/Al molar ratio of 25 and 50, respectively. To assess the hydrothermal stability, ASM25 and ASM50 were boiled in 100 °C

* Corresponding author. Fax: +86 351 4041153.
E-mail address: xuyao@sxicc.ac.cn (Y. Xu).

0022-4596/$ - see front matter © 2008 Elsevier Inc. All rights reserved.
doi:10.1016/j.jssc.2008.05.046

water for 300 h. The boiled samples were noted as ASM25H and ASM50H. A reference sample HZSM-5 (Si/Al ratio 25) was synthesized according to [14].

All the samples were characterized by small-angle X-ray scattering (SAXS, 4B9A beamline at the Beijing Synchrotron Radiation Facility), TEM (JEOL 100CX). The contact angle for water of the tabletting sample was measured by a contact-angle meter (CA-A, Kyowa, Japan).

N_2 adsorption/desorption isotherms were obtained at −196 °C on a Tristar 3000 Sorptometer, using static adsorption procedures. Samples were degassed at 150 °C and 10^{-6} Torr for 12 h prior to analysis. BET surface area was calculated from the linear part of the BET plot according to IUPAC recommendations. Pore size distribution was calculated by the Barrett–Joyner–Halenda (BJH) model.

^{29}Si MAS NMR and ^{27}Al MAS NMR spectra were measured on a UNITY INOVA-500 spectrometer using a DOTY Scientific multinuclear probe and 5 mm zirconia rotors. ^{29}Si resonance frequency, 99.745 MHz; pulse width, 4 μs; recycle delay time, 400 s; spinning frequency, 8 kHz; and tetramethylsilane were used to assign 0 chemical shift. ^{27}Al resonance frequency, 130.245 MHz; pulse width, 1 μs; recycle delay time, 1 s; spinning frequency, 4 kHz; and $Al(H_2O)_6^{3+}$ were used to assign 0 chemical shift.

Temperature-programmed desorption of ammonia (NH_3-TPD) was performed in a quartz micro-reactor. A 0.20 g of sample was freshly heated in argon at 600 °C for 0.5 h. NH_3 was then introduced to the sample after it was cooled down to 120 °C. To remove the weakly adsorbed NH_3, the sample was swept using argon at 120 °C for 2 h. The TPD experiment was then carried out in argon with a carrier-gas flowing rate of 40 mL min^{-1} from 120 to 600 °C using a heating rate of 10 °C min^{-1}. The NH_3 desorption was detected by Shimadzu GC-9A equipped with a TCD detector.

1,3,5-Triisopropylbenzene (TPB) cracking over ASM25, ASM50 and HZSM-5 was carried out at 300 °C by pulse method to evaluate catalytic performance of the samples. The cracking experiment over HZSM-5 was only for a comparison with those two samples. In each run, 0.2 μL reactant was pulsed and cracked over 0.06 g of catalyst, and nitrogen was used as the carrier gas at a flowing rate of 50 mL min^{-1}. The reaction products were analyzed using GC-9A (Shimadzu Co.) equipped with a FID detector and a high-resolution Chrom-Workstation Data Set. GC was used to determine the reactant conversion.

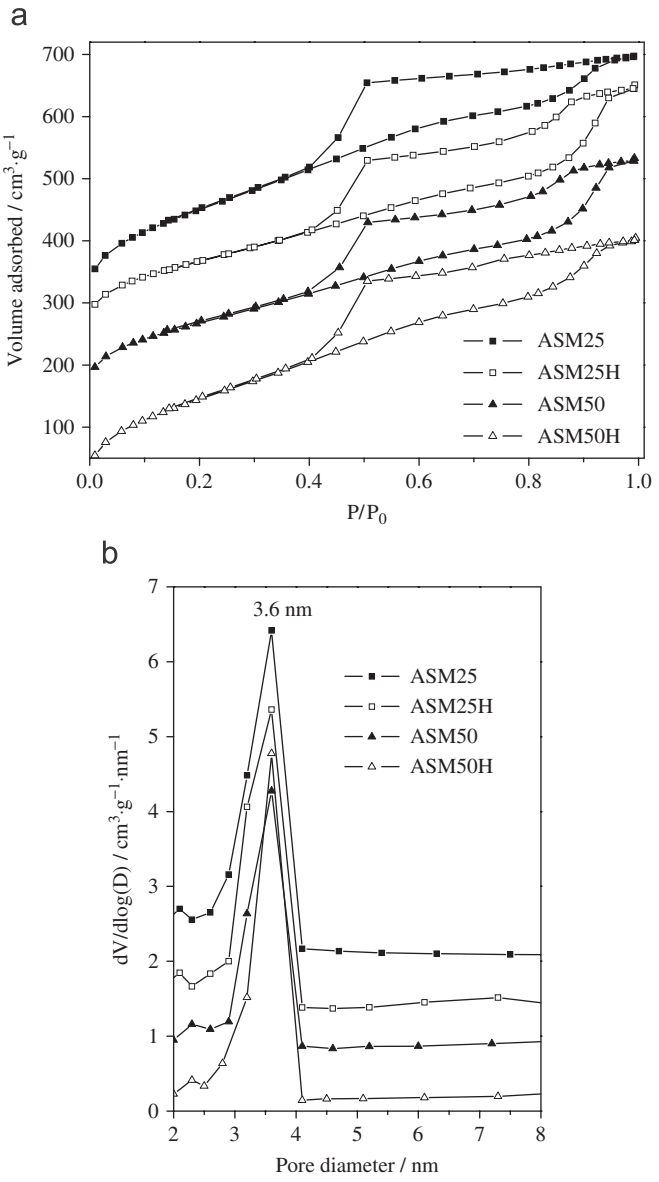

Fig. 1. (a) N_2 adsorption–desorption isotherms and (b) BJH pore size distributions of mesoporous aluminosilicates.

3. Results and discussion

3.1. Structure analysis

Fig. 1a shows the N_2 adsorption–desorption isotherms of the obtained samples. In Fig. 1, the isotherms all exhibit a typical adsorption curve of type-IV with a type H2 hysteresis loop which is attributed to the presence of pores with narrow mouths (ink-bottle pores) [15]. Fig. 1b shows the corresponding BJH pore size distributions (calculated from the BJH model). All samples exclusively show a narrow pore size distribution centered at 3.6 nm, which were very different from the results of bimodal micro/mesoporous materials without Al additive reported in our previous work [12]. It can be seen from Fig. 1 that as-synthesized mesoporous aluminosilicates have nearly the same adsorption–desorption isotherms and the same pore size distributions as those boiled ones. Table 1 summarizes the texture parameters of ASM25 and ASM50 before and after hydrothermal treatment. After 300 h hydrothermal treatment, the surface area and pore volume of ASM25 changed from 588 to 564 $m^2 g^{-1}$ and from 0.61 to 0.63 $cm^3 g^{-1}$, respectively. Those of ASM50 changed from 453 to 450 $m^2 g^{-1}$ and from 0.59 to 0.62 $cm^3 g^{-1}$, respectively. These results indicate that ASM25 and ASM50 all show excellent hydrothermal stability.

Table 1
The texture parameters and contact angle for water

Sample	Si/Al molar ratio	Surface area ($m^2 g^{-1}$)	Pore volume ($cm^3 g^{-1}$)	Contact angle for water (deg)
ASM25	25	588	0.61	128
ASM25H	25	564	0.63	131
ASM50	50	453	0.59	147
ASM50H	50	450	0.62	145

The SAXS results of ASM25 and ASM25H are shown in Fig. 2. Sample ASM25 presents an obvious diffractive peak at $q = 1.304\ nm^{-1}$ from which a periodic length of $d = 4.82$ nm can be calculated by formula $d = 2\pi/q$. Compared to sample ASM25,

sample ASM25H presents a slightly weakened and widened diffractive peak at $q = 1.324\,nm^{-1}$ corresponding to a periodic length of $d = 4.75\,nm$. Therefore the mesoporous structure was kept well after boiling treatment. From the TEM image (Fig. 3a) of ASM25, wormlike mesopores cover nearly all the view field of samples. Measured from TEM image, the average pore diameter of ASM25 is about 3.5 nm and the average pore wall thickness is about 1.3 nm. These two results are in good agreement with that from SAXS experiment. Fig. 3b shows the TEM image of boiled sample ASM25H, from which the pore structure after hydrothermal treatment has little change compared with the as-synthesized ASM25. This TEM image visibly confirmed the results obtained from N_2 adsorption/desorption experiments (Fig. 1).

The ^{27}Al MAS NMR spectra of ASM25 and ASM50 (Fig. 4a) only exhibit single chemical shifts at 49.1 ppm that can be assigned to four-coordinated Al, indicating that Al atoms were incorporated in the frameworks of the obtained mesoporous aluminosilicates. The ^{27}Al MAS NMR spectrum of boiled sample ASM25H is also shown in Fig. 4a. Similar to the other two samples, only four-coordinated Al signal can be observed with respect to ASM25H, and no obvious changes in the ^{27}Al NMR signal intensity and position can be found from the comparison between ASM25H and ASM25. Therefore, the chemical situation of Al atoms was maintained after hydrothermal treatment, which is in agreement with the results of N_2 adsorption/desorption experiments. If the mesoporous structures were destroyed obviously during the hydrothermal treatment, there would be detectable six-coordinated Al atoms evolved from original four-coordinated Al. Fig. 4b shows the ^{29}Si MAS NMR spectra of ASM25 and ASM25H, in which there are five distinct signals at −110, −103, −65, −56 and 12 ppm. The two resonance peaks at −110 and −103 ppm can be attributed, respectively, to $Si*(OSi)_4$ (Q^4) and $(HO)Si*(OSi)_3$ (Q^3) that belong to those silicon atoms introduced by the hydrolyzation and polycondensation of TEOS [16]. The signals at –65 and –56 ppm are corresponding, respectively, to $CH_3Si*(OSi)_3$ (T^3) and $CH_3Si*(OH)(OSi)_2$ (T^2) that belong to the silicon atoms in PMHS chains [17]. The low-field peak at 12 ppm can be assigned to $(CH_3)_3Si*OSi$ (M^1) that belong to the silicon atoms located at the two ends of PMHS chain [18]. The appearance of T^3, T^2, and M^1 NMR signals indicates that PMHS and TEOS have jointly condensed and CH_3 groups have been introduced into the materials. But there are some small differences between the two ^{29}Si MAS NMR spectra. From Fig. 4b, the T^2 shoulder peak disappeared in the curve ASM25H and the Q^3 shoulder peak

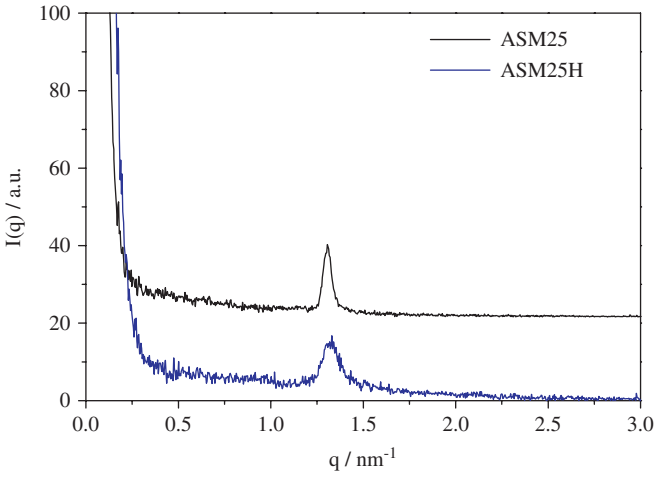

Fig. 2. The small-angle X-ray scattering (SAXS) of ASM25 and ASM25H.

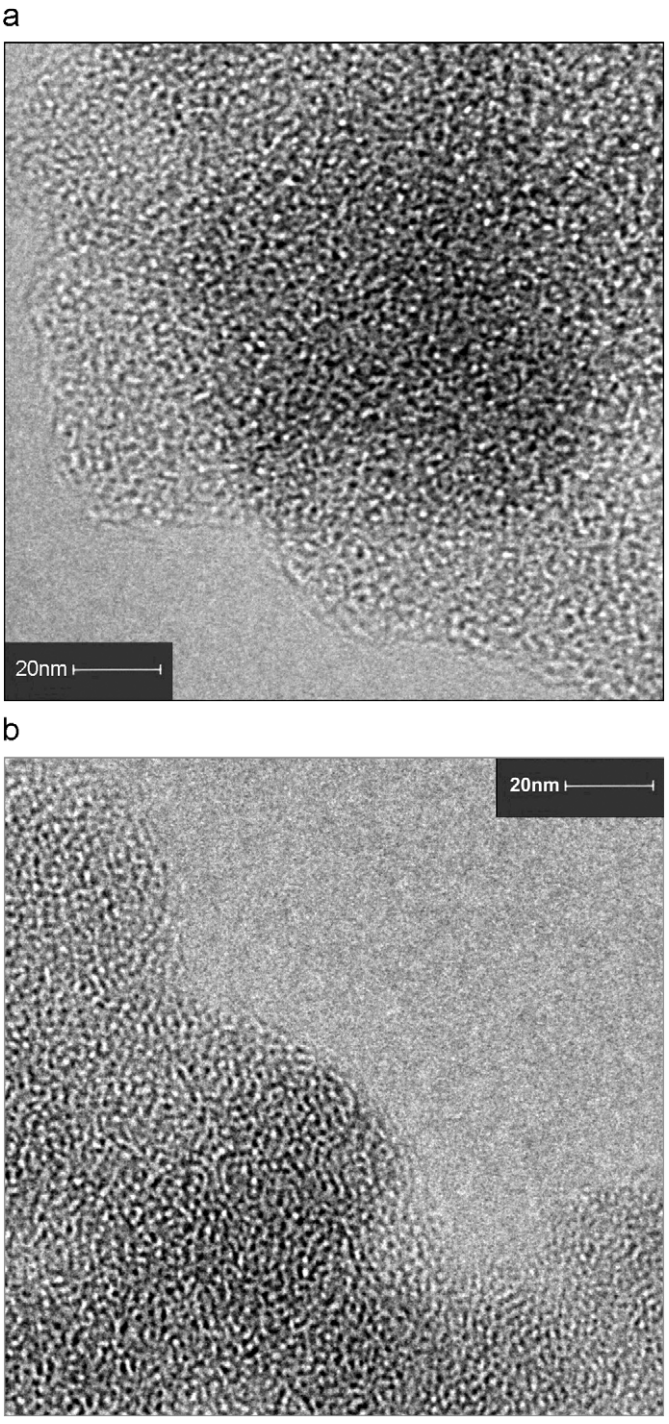

Fig. 3. TEM images of (a) ASM25 and (b) ASM25H.

became far weaker than that of ASM25, indicating the condensation of Si-OH groups was more complete after hydrothermal treatment. This is easy to be understood because the incompletely condensed Si-OH groups would continue to condense in hot water.

3.2. Acidity and hydrophobicity

Due to the existence of large amount of CH_3 groups, the mesoporous aluminosilicates obtained good hydrophobicity. The

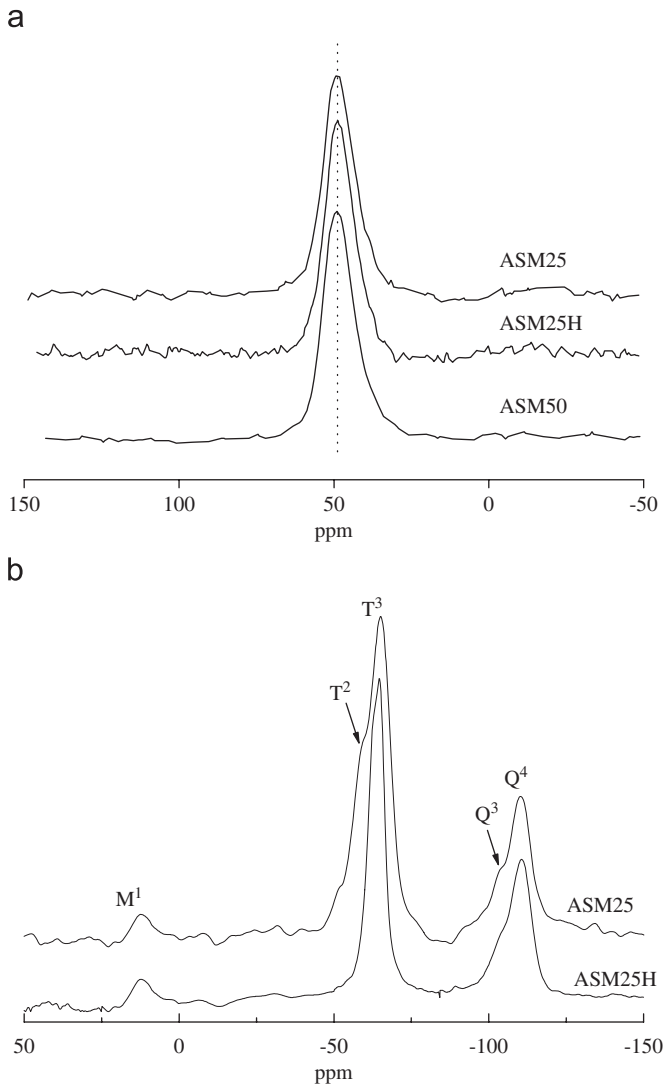

Fig. 4. (a) ^{27}Al MAS NMR spectra of ASM25, ASM25H and ASM50 and (b) ^{29}Si MAS NMR spectra of ASM25 and ASM25H.

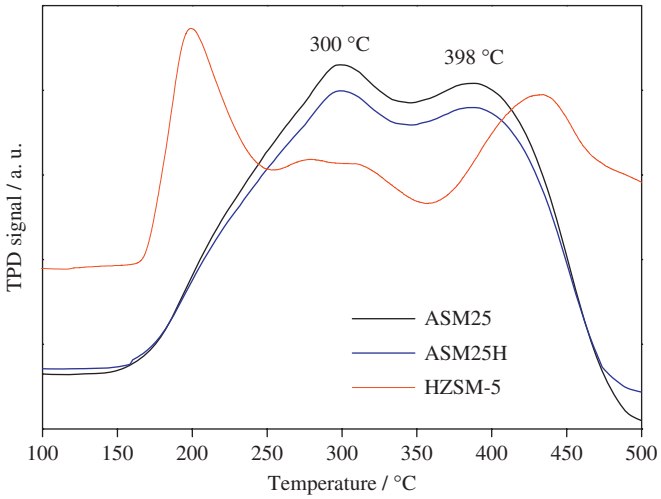

Fig. 5. NH_3-TPD profiles for ASM25, ASM25H and HZSM-5.

contact-angle data of tableted sample for water are collected in Table 1. ASM50 with higher Si/Al (more Si-CH_3 groups) possessed better hydrophobicity than ASM25. Even after treatment in boiled water, the samples still possessed good hydrophobicity because the Si-CH_3 could not be destroyed under the present experimental conditions.

The acidity of ASM25 and ASM50 was characterized by NH_3-TPD and the results were shown in Fig. 5. Two NH_3 desorption peaks at 300 and 398 °C, corresponding to medium acidity and strong acidity, respectively, can be clearly observed for the samples ASM25 and ASM25H, which is different from that of HZSM-5 zeolite and H-Beta zeolite [2]. It also can be seen that the acid amount of ASM25H is slightly smaller than that of ASM25. Therefore, after 300 h boiling treatment the content of aluminium in mesoporous aluminosilicates can be mostly kept well. Furthermore, ASM25 possesses obviously more acid amount than ASM50 due to the lower Si/Al ratio (NH_3-TPD result is not listed here). The NH_3-TPD result of lab-prepared HZSM-5 with Si/Al ratio of 25 was also shown in Fig. 5 from which two strong NH_3 desorption peaks could be identified at 200 and 432 °C. As all known, HZSM-5 zeolite was a very important catalyst with strong acidity that has been applied in high hydrocarbon cracking. Its catalytic performance will be compared with the samples obtained in this work.

3.3. Catalytic performance

Generally the cracking of TPB (molecular diameter ~0.94 nm) needs catalysts with medium acidity [19]. The catalytic performance for TPB cracking over the mesoporous aluminosilicates obtained in this work is listed in Table 2. Obviously ASM25 and ASM50 all exhibited high conversion capability of 100% and 89.56%, respectively. The higher conversion of ASM25 should be attributed to the higher aluminium content. Apart from the slightly different conversion capabilities, the selectivity of products was different between ASM25 and ASM50. Over ASM50, the selectivity of propylene (the final cracking product) was higher (45.72%) than that over ASM25 (21.09%). And, there were no diisopropylbenzene produced over ASM50 in contrast to ASM25. For a comparison, the TPB cracking performance is also listed in Table 2. Only 36.47% of TPB reactant could be converted and diisopropylbenzene (an initiative cracking product) was the main product. Because of the small micropore diameter of HZSM-5 (ranged in 0.51–0.56 nm) relative to TPB molecule, the reactant TPB cannot go into micropores, leading to the acid position on the inner surface of HZSM-5 cannot be utilized in the catalysis. Therefore HZSM-5 exhibited the worst catalytic performance for TPB cracking, as shown in Table 2. Owing to the large pore and the strong acidity provided by the uniform four-coordinated Al of ASM samples, the excellent catalytic performance for TPB cracking was acquired easily.

4. Conclusion

Through a nonsurfactant route based on PMHS–TEOS–AIP co-polycondensation, hydrothermally stable mesoporous aluminosilicates were successfully prepared. Taking the strong acidity of mesoporous aluminosilicates into consideration, these materials may be useful for cracking heavy hydrocarbon.

Table 2
Catalytic performance for 1,3,5-triisopropylbezene cracking

Samples	Conversion (%)	Products distribution (%)			
		Propylene	Benzene	Isopropylbenzene	Diisopropylbenzene[a]
ASM50	89.56	45.72	4.74	49.54	0
ASM25	100	21.09	46.65	31.11	1.15
HZSM-5	36.47	22.05	–	22.56	55.39

[a] Total selectivity of *m*-diisopropylbenzene and *p*-diisopropylbenzene.

Acknowledgments

Financial supports from the National Natural Science Foundation of China (No. 20573128), and State Key Program for Development and Research of China (2005CB221402) and Australian Research Council are gratefully acknowledged.

References

[1] A. Corma, Chem. Rev. 97 (1997) 2373.
[2] Z.T. Zhang, Y. Han, F.S. Xiao, S.L. Qiu, L. Zhu, R.W. Wang, Y. Yu, Z. Zhang, B.S. Zou, Y.Q. Wang, H.P. Sun, D.Y. Zhao, Y. Wei, J. Am. Chem. Soc. 123 (2001) 5014.
[3] R. Mokaya, Angew. Chem. Int. Ed. 38 (1999) 2930.
[4] R. Mokaya, W. Jones, Chem. Commun. (1998) 1839.
[5] R. Mokaya, Chem. Commun. (2001) 633.
[6] R. Mokaya, Chem. Phys. Chem. 3 (2002) 360.
[7] Y. Liu, W. Zhang, T.J. Pinnavaia, J. Am. Chem. Soc. 122 (2000) 8791.
[8] Y. Liu, W. Zhang, T.J. Pinnavaia, Angew. Chem. Int. Ed. 40 (2001) 1255.
[9] Z.T. Zhang, Y. Han, L. Zhu, R.W. Wang, Y. Yu, S.L. Qiu, D.Y. Zhao, F.S. Xiao, Angew. Chem. Int. Ed. 40 (2001) 1258.
[10] J.L. Zheng, Y. Zhang, Z.H. Li, W. Wei, D. Wu, Y.H. Sun, Chem. Phys. Lett. 376 (2003) 136.
[11] D.J. Yang, Y. Xu, S.R. Zh, J.L. Zh, J.P. Li, D. Wu, Y.H. Sun, Chem. Lett. 34 (2005) 1138.
[12] D.J. Yang, J.P. Li, Y. Xu, D. Wu, Y.H. Sun, H.Y. Zhu, F. Deng, Micropor. Mesopor. Mater. 95 (2006) 180.
[13] D.J. Yang, Y. Xu, D. Wu, Y.H. Sun, J. Phys. Chem. C 111 (2007) 999.
[14] H. Lechert, R. Kleinwort, Verified Synthesis of Zeolitic Materials, second ed., Elsevier, Amsterdam, 2001, p. 199.
[15] M. Kruk, M. Jaroniec, Chem. Mater. 13 (2001) 3169.
[16] E. Prouzel, T.J. Pinnavaia, Angew. Chem. Int. Ed. 36 (1997) 516.
[17] C.J. Brinker, G.W. Scherer, Sol–Gel Science: The Physics and Chemistry of Sol–Gel Processing, Academic Press, San Diego, 1990, pp. 160–173.
[18] T.I. Suratwala, M.L. Hanna, E.L. Miller, P.K. Whitman, I.M. Thomas, P.R. Ehrmann, R.S. Maxwell, A.K. Burnham, J. Non-Cryst. Solids 316 (2003) 349.
[19] H. Koch, W. Reschetilowski, Micropor. Mesopor. Mater. 25 (1998) 127.